



microwave JOURNAL®

COMPARISON OF COAXIAL DIPOLE ANTENNAS FOR APPLICATIONS IN THE NEAR-FIELD AND FAR-FIELD REGIONS

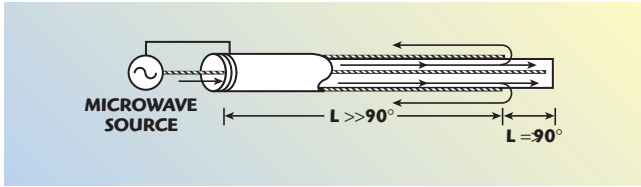
Coaxial antennas with properties similar to those of a two-wire dipole antenna are presented and analyzed. Since coaxial antennas extend along a straight line and can have almost any radius, they may be easily inserted into confined spaces that require an antenna. Coaxial antennas are easy to construct, naturally adapted to a coaxial input connection, thus avoiding the use of a balun (a balanced to unbalanced adapter), and avoid using a T-shaped structure (as for the two-wire dipole). By altering in specific ways the inner and outer conductors of a 50 Ω transmission line, four different coaxial antennas are formed that have characteristics similar to those of a two-wire dipole antenna. These antennas are compared and discussed, while noting the similarities and differences between them and the two-wire dipole antenna. The antenna parameters determined are the near-field and far-field radiation patterns, the input impedance and the input reflection coefficient (S_{11}). The antennas are modeled using a high frequency structure simulator (HFSS), then constructed and their properties measured to confirm the calculations and simulations.

Coaxial antennas with properties similar to those of a two-wire dipole antenna are developed and analyzed in this article. In order to simulate the characteristics of a two-wire dipole antenna with a 50 Ω coaxial line, the inner and outer conductors of the coaxial line are altered in specific ways. It is advantageous in certain applications to use such coaxial line antennas rather than a two-wire dipole antenna. Coaxial antennas are easy to construct, naturally adapted to a coaxial input connection, thus avoiding the use of a

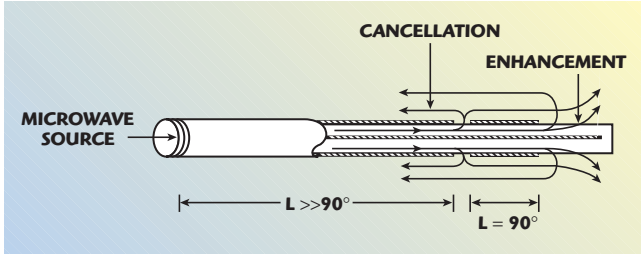
balun (a balanced to unbalanced adapter), and avoid using a T-shaped structure (as for the two-wire dipole). Since coaxial antennas extend along a straight line and can have almost any radius, they may be easily inserted into confined spaces that require an antenna. For example, in cancer therapy, the cancerous region may be heated by microwaves using an

BRIAN DROZD AND WILLIAM T. JOINES
*Duke University
Durham, NC*

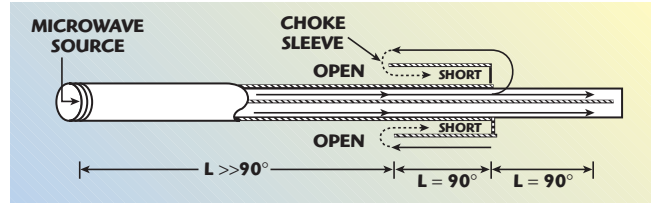
TECHNICAL FEATURE



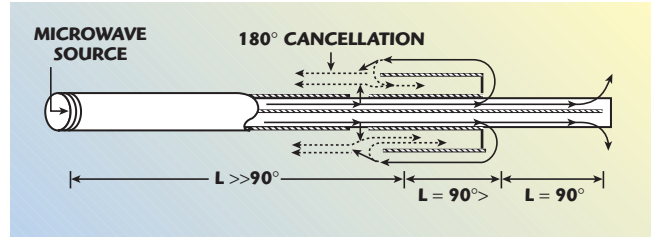
▲ Fig. 1 Diagram of antenna 1 showing the quarter-wavelength (90° electrical length) extended inner-conductor coaxial line.



▲ Fig. 2 Diagram of antenna 2 with a gap in the outer conductor.



▲ Fig. 3 Diagram of antenna 3 with a $\lambda/4$ choke sleeve.



▲ Fig. 4 Diagram of antenna 4 with both a choke sleeve and a $\lambda/4$ spaced back gap.

interstitial or intercavitary antenna, especially in the case of brain or prostate tumors. Coaxial antennas also have applications in wireless communications; the monopole antenna used on mobile telephones is similar to one of the coaxial antennas discussed herein.

The measured and simulated results of the coaxial dipole antennas approximate the characteristics of the two-wire dipole, especially in terms of radiation pattern. Thus, the standard two-wire dipole antenna is presented to serve as a basis for comparison with the coaxial dipole antennas. Four types of coaxial antennas were constructed. The first type of coaxial antenna (antenna 1) was made by simply stripping off the outer conductor to extend the inner conductor by a quarter-wavelength and is shown in **Figure 1**. This antenna (referred to as the extended inner conductor antenna) is analyzed and measured to show that simply removing part of the outer conductor is not enough to adequately simulate a standard dipole antenna. A series of additional structural changes are made to make coaxial dipole antennas with radiation patterns that more closely approximate the standard dipole pattern.

For the next coaxial antenna (antenna 2), a small gap in the outer conductor, spaced a quarter-wavelength back from the end of the coaxial line, is added to the simple extended inner conductor antenna. Its cross-section is shown in **Figure 2**. This gap serves to cancel waves traveling back toward the source, and the resulting radiation

pattern approximates that of the standard dipole. This antenna is referred to as the quarter-wavelength back-gap antenna. The third type of coaxial antenna (antenna 3) is made by adding a quarter-wavelength choke sleeve to the quarter-wavelength extended inner conductor coaxial antenna, which also prevents wave propagation back along the outer conductor. Its cross-section is shown in **Figure 3**. This antenna is referred to as the quarter-wavelength choke-sleeve antenna. Finally, the fourth coaxial antenna (antenna 4) modifies the quarter-wavelength extended inner conductor coaxial antenna by having both a choke-sleeve and a quarter-wavelength spaced back-gap. This final version is shown in **Figure 4** and is referred to as the back-gap choke-sleeve antenna. These antennas are compared and discussed, noting the differences between them and the two-wire dipole antenna. The antenna parameters determined are the radiation pattern, the input impedance and the input reflection coefficient (S_{11}). The antennas are modeled using a high frequency structure simulator (HFSS). In addition to the simulations generated, the coaxial antennas are constructed and their properties are measured to confirm the calculations and simulations.

HALF-WAVELENGTH DIPOLE STANDARD

A half-wave dipole antenna is used as a standard of comparison. Two important properties of the finite-length,

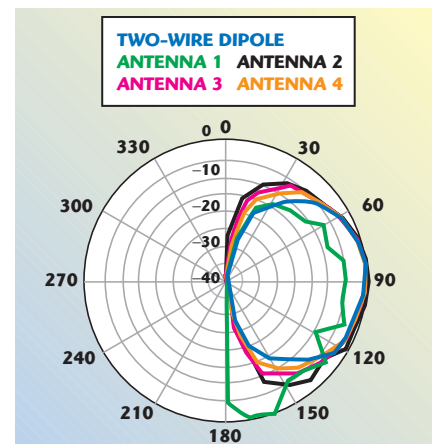
center-fed dipole antenna are the radiation pattern and the input impedance. The radiated electric field is found through Maxwell's equations, and in the far-field it is given by¹

$$E_{\theta} = j\eta I \frac{e^{-j\beta r}}{2\pi r} \frac{\cos\left[\frac{\pi}{2} \cos\theta\right]}{\sin\theta} \quad (1)$$

where

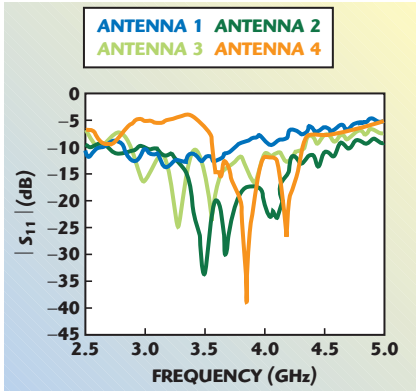
- I = the antenna current flow
- $\eta = 377 \Omega$
- r = distance from the dipole
- θ = the polar angle

The distance to the far-field of an antenna is given by the approximate expression,¹ $r_{\text{far}} \approx 2D^2/\lambda$, where D is the largest dimension of the antenna and λ is wavelength. Thus, for the $\lambda/2$ dipole, $r_{\text{far}} \approx \lambda/2$. Due to the approximate nature of the expression cited



▲ Fig. 5 HFSS simulation of the far-field radiation patterns of all five antennas at 3.5 GHz.

TECHNICAL FEATURE



▲ Fig. 6 Measured input reflection coefficient S_{11} for all coaxial antennas.

the near-field will be considered to be in the region $r \leq \lambda/2$ and the far-field to be in the region $r \geq \lambda$.

The far-field radiation pattern for the two-wire dipole and all of the coaxial antennas, determined using HFSS, are shown in **Figure 5**. In this figure, the normalized magnitude of the electric field versus angle θ is shown with θ varying from 0° to 180° . A 360° azimuthal rotation of this pattern yields a full 3-D doughnut-shaped pattern, in full agreement with equation (1-1). The two-wire dipole shows a circular-shaped pattern with maximum directivity occurring at $\theta \gg 90^\circ$, as expected.

The near-field of a dipole antenna has a distribution of electric field intensity that is very different from that given in Equation 1 for the far-field. In the near-field, the electric field intensity has components in both the radial (r) direction and the θ direction given by⁸

where

$p = Ih/(j\omega)$ is the electric dipole moment

h = the dipole length

ω = the radian frequency

ϵ = the permittivity of the surrounding region

(for air, $\epsilon = \epsilon_0 = 8.854 \text{ pF/m}$)

Thus, the near-field drops off very rapidly with distance and is larger along the polar axis of the antenna where θ is 0° or 180° . For comparison purposes the near field-field will be simulated using HFSS for each antenna, but not measured.

EXTENDED INNER CONDUCTOR COAXIAL ANTENNA

Antenna 1 is constructed by simply stripping off the outer conductor of a

regular coaxial line to extend the inner conductor by a quarter-wavelength. This antenna does not emulate a standard dipole antenna, but it forms the starting point that is used for each of the three later coaxial dipole antennas. Thus, its properties are important to note in order to show how each additional modification serves to shape the near-field and far-field radiation patterns. For this basic structure, the wave propagates along the coaxial line and divides at the open end. Part of the wave continues along the extended inner conductor, and the other part travels back toward the source on the outside of the coaxial outer conductor. Thus, while energy will be radiated from the quarter-wavelength extended inner conductor, there will also be radiation from the outer conductor that is distributed over much more than a quarter-wavelength.

The wave traveling along the outside of the outer conductor of the coaxial line is a surface wave. The electric field lines emanating from positive charges and terminating on negative charges are distributed approximately sinusoidally along the outer conductor. These field lines also form a radiating structure, and as the wave propagates along the outer conductor the antenna radiation pattern is pulled downward toward the source, as shown by the simulation. The maximum directivity of the pattern is seen to occur near $\theta = 160^\circ$. The full radiation pattern is obtained by rotating it through 360° about the vertical axis.

Experimental Results for the Extended Inner Conductor Antenna

In constructing the extended inner conductor antenna, Styrofoam spacers were used to keep the inner conductor in the center of the air-filled coaxial line. The measurements were made using the constructed coaxial antenna as the transmitting antenna, and the receiving antenna was a microstrip dipole that functioned well over the frequency range of interest. A network analyzer (HP 8720C) served as both the transmitting source and the receiving detector. The transmitting and receiving antennas were placed inside a small (two feet on each side) anechoic chamber made of two-inch thick absorbing material (Eccosorb). The anechoic chamber served to minimize outside inter-

ference as well as reflections from other objects nearby.

The magnitude of the input reflection

$$E = \sqrt{E_r^2 + E_\theta^2}$$

$$= p \frac{e^{-j\beta r}}{4\pi\epsilon r^3} \sqrt{1 + 3\cos^2 \theta} \quad (2)$$

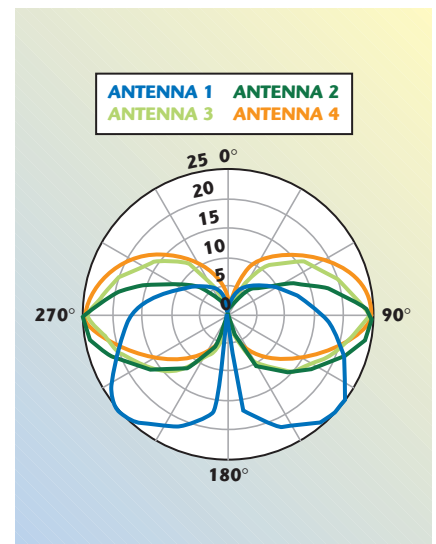
coefficient (S_{11}), expressed in dB, is $S_{11} \text{ (dB)} = 20\log|S_{11}|$, which is a negative quantity since $|S_{11}| < 1$. The return loss (RL) in dB is

$$\text{RL (dB)} = -S_{11} \text{ (dB)} = 10\log|S_{11}|^2 \quad (3)$$

since $|S_{11}|^2$ is the ratio of power reflected to power incident upon the antenna input. For 10 percent reflected power, $|S_{11}|^2 = 0.1$, $S_{11} \text{ (dB)} = -10 \text{ dB}$ and $\text{RL (dB)} = 10 \text{ dB}$. For 1 percent reflected power, $|S_{11}|^2 = 0.01$, $S_{11} \text{ (dB)} = -20 \text{ dB}$ and $\text{RL (dB)} = 20 \text{ dB}$.

Assuming no losses, the remainder of the incident power (the part not reflected) is radiated. For measuring S_{11} , or the return loss in dB, the coaxial antenna is placed in the anechoic chamber while connected to the network analyzer. For the extended inner conductor antenna (antenna 1), the measured return loss is approximately 10 dB from 2.5 to 3.7 GHz, as shown in **Figure 6**. For this antenna and all of the others that are discussed and compared, no attempt was made to reduce reflected power by matching the input impedance to the 50Ω source.

The measured radiation pattern for the extended inner conductor antenna is shown in **Figure 7**. The electric far-field at each point, a set dis-



▲ Fig. 7 Measured far-field radiation pattern for all coaxial antennas.

TECHNICAL FEATURE

tance away from the antenna, was measured and recorded. The radiation pattern for this antenna shows that a considerable amount of energy in the wave is traveling back towards the source along the outer conductor, thus producing a maximum in directivity at $\theta = 135^\circ$ instead of at $\theta = 90^\circ$.

COAXIAL DIPOLE ANTENNA 2 WITH A GAP SPACED A QUARTER-WAVELENGTH BACK

The previous section shows that the extended inner conductor coaxial antenna does not behave as a normal dipole antenna because an excessive amount of energy is radiated back along the outer conductor. However, adding a gap in the outer conductor (antenna 2) that is spaced a quarter-wavelength back from the extended inner conductor, makes the radiation pattern of the coaxial antenna very similar to that of a two-wire dipole antenna. The gap in the outer conductor limits the amount of current or signal power that flows back toward the source past the quarter-wavelength section of the outer conductor so that microwave power is concentrated along two quarter-wavelength conductive sections at the radiating end.

To demonstrate how cancellation and enhancement occur, the path of the wave of energy from the source is traced in the diagram of antenna 2. The wave of energy from the source travels up the coaxial line to the gap in the outer conductor. Part of this source energy travels out of the gap and onto the outer conductor, and the other part continues along the quarter-wavelength region between the inner and outer conductors. The part that continues inside the coaxial line divides two ways upon reaching the end of the outer conductor. One part of this energy radiates into the space surrounding the extended inner conductor, and the other part travels back down the outside of the outer conductor a quarter-wavelength. The latter combines 180° out of phase with the wave that leaked out through the gap originally. The size of the gap allows these two surface-guided waves to have similar amplitudes and they tend to cancel each other, so that radiation back down the outer conductor toward the source is minimized or eliminated.

Simulated Results for the Quarter-wavelength Back-gap Antenna Using HFSS

The aforementioned gap in the outer conductor makes the pattern of electric field intensity on and near conductors similar to that of the two-wire dipole antenna. This is the electric field intensity in the near-field due to the charge and current distribution on conductors, as shown in *Appendix A*, where the back-gap antenna is on the left and the extended inner conductor antenna is on the right. As seen in this comparison, the wave traveling back down the outer conductor is practically eliminated by the gap in the outer conductor. Thus, the electric field lines in the near-field region closely surrounding the antenna are mostly confined to the half-wavelength region at the end of the antenna. On the other hand, the near-field electric field intensity for the extended inner conductor antenna (no gap) clearly extends back along the outer conductor toward the source.

The circular-shaped normalized radiation pattern simulated using HFSS for the coaxial antenna with a gap spaced a quarter-wavelength back from the end of the outer conductor is shown in a previous figure. It is seen that an almost circular-shaped pattern is obtained, and maximum directivity occurs at $\theta = 90^\circ$, as it does for the two-wire dipole antenna.

Experimental Results for the Quarter-wavelength Back-gap Antenna (Antenna 2)

The measured S_{11} for antenna 2 is shown in a previous graph. At the design frequency of 3.5 GHz, the return loss is 33.75 dB. This antenna is fairly broadband, with a bandwidth of 800 MHz between points where $S_{11} \leq -15$ dB.

The measured radiation pattern for this antenna has been shown for a vertical orientation of the antenna. The measured field pattern agrees reasonably well with the HFSS simulation. Both patterns approximate the doughnut-shaped radiation pattern that is characteristic of the two-wire dipole. This constructed antenna has a small amount of wave energy traveling down the outer conductor towards the microwave source, which is not cancelled out by the gap. Still, this antenna is a vast improvement

over the extended inner conductor antenna in terms of radiation pattern and making the $\lambda/2$ end a more effective radiator.

COAXIAL ANTENNA WITH QUARTER-WAVE CHOKE SLEEVE (ANTENNA 3)

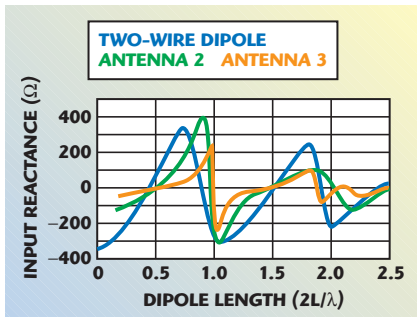
An alternative way of making a coaxial antenna that also simulates the best features of the two-wire dipole is to place a quarter-wavelength choke sleeve around the outer conductor. Due to the shorted end of the choke sleeve, an open circuit is presented to a microwave signal that would travel back along the choke sleeve toward the source. This tends to confine the radiating source to the half-wavelength region between the open end of the choke sleeve and the extended inner conductor of the coaxial line. From the end of the coaxial line, part of the wave radiates outward from the extended inner conductor, and another part radiates from the quarter-wavelength choke-sleeve section that presents an open circuit on the end.

HFSS Simulation Results for the Choke-sleeve Antenna

The electric field lines in the near-field of the choke-sleeve coaxial antenna are similar to what would be expected for the near-field lines of the two-wire dipole. From this HFSS simulation, the magnitude of charge distribution (electric field intensity) on conductors is shown in *Appendix B* for the choke-sleeve antenna (left) and (for comparison) the extended inner conductor antenna (right). Thus, in the region immediately surrounding the choke-sleeve antenna, the magnitude of the electric field varies in an apparent sinusoidal manner with a minimum where the extended inner conductor begins and maximum points on each leg of the antenna. It is again quite clear that the simple extended inner conductor antenna has a significant propagation of energy back toward the source on the outer conductor, whereas very little of the wave energy travels along the outer conductor past the open end of the choke sleeve.

The simulated far-field radiation pattern for this antenna, obtained using HFSS, has been shown previously and approximates the two-wire di-

TECHNICAL FEATURE



▲ Fig. 8 Simulated input reactance of a two-wire dipole antenna and antennas 2 and 3.

pole's 2-D circular shape. The radiation pattern is tilted slightly upward, so that maximum directivity occurs at $\theta = 90^\circ$. This upward tilt is probably due to the necessarily larger radius of the choke sleeve fitted around the outer conductor.

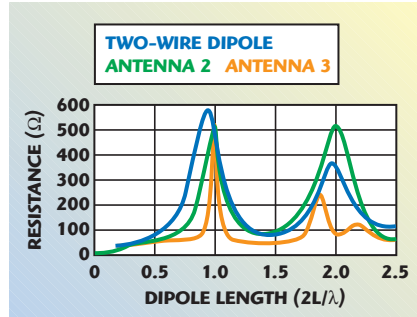
Experimental Results for the Choke-sleeve Antenna

The measurements of S_{11} in dB versus frequency for a constructed choke-sleeve antenna confirm that this antenna is an improvement over the previous unaltered, quarter-wavelength extended inner conductor antenna. The S_{11} of the choke-sleeve antenna shows that at the design frequency of 3.5 GHz (where each leg is $\lambda/4$ in length) the input reflection (S_{11}) is -25 dB. On the other hand, this antenna had a relatively narrow bandwidth of 100 MHz.

The measured radiation pattern for this antenna has been shown in a previous graph. This pattern is similar to the doughnut shape of the two-wire dipole, and is in agreement with the HFSS simulation in exhibiting the slight upward tilt of the pattern. However, the measured pattern is noticeably flatter than the simulation. This is probably due to measurement error, since the detector on the receiving antenna is less sensitive to the lower field values in the polar regions.

COAXIAL ANTENNA WITH QUARTER-WAVELENGTH CHOKE SLEEVE AND ADJACENT GAP (ANTENNA 4)

The rationale for fitting the coaxial antenna with a choke sleeve and a quarter-wavelength spaced back-gap is similar to that of the previous sections. It would be interesting to know if further improvements can be obtained by combining the choke sleeve (better ra-



▲ Fig. 9 Simulated input resistance of a two-wire dipole antenna and antennas 2 and 3.

diation pattern) with the back-gap (better return loss). Adding a choke sleeve to the quarter-wavelength spaced back-gap antenna should result in a further reduction of the current traveling back toward the source along the outer conductor, and thus, an improvement in the radiation pattern may occur. In a manner similar to previous diagrams, the wave from the microwave source travels from left to right, radiates from the quarter-wavelength outer sections and interacts with other parts of the wave.

As illustrated earlier, the gap serves to cancel 180° out of phase parts of the wave on the outer conductor. There is a part that travels past the choke sleeve on the outer conductor that has been delayed by approximately 180° more than a part that leaks through the gap and travels toward the source. The size of the gap should be such that the amplitude of the wave that leaks onto the outer conductor from the choke sleeve is equal to the amplitude of the wave that leaks out of the gap.

HFSS Simulation Results for the Choke-sleeve, Back-gap Antenna

The normalized far-field radiation pattern obtained from the HFSS simulation has been shown previously. The antenna was placed along the $\theta = 0^\circ$ axis and points of the radiation pattern were simulated by varying θ from 0° to 180° . A radiation pattern very similar to that of the two-wire dipole is observed.

Measured Results of the Choke-sleeve, Back-gap Antenna

This antenna was constructed and measurements were taken. First, S_{11} for this antenna was measured by the network analyzer and plotted, as shown in a previous figure. As seen, the frequency for minimum reflec-

tion (maximum radiation) is 3.86 GHz, where S_{11} is 40 dB down. At the design frequency of 3.5 GHz, S_{11} is approximately 7 dB down. This upward frequency shift of approximately 0.36 GHz is probably due to interactions between the choke sleeve and the back-gap. Clearly, the choke sleeve will alter the wave energy that reaches the gap by traveling along the outer conductor. Therefore, some further optimization of dimensions will be needed to center the response at 3.5 GHz.

The far-field radiation pattern of this antenna was closer to that of the two-wire dipole than any of the previous antennas. This is probably because the wave traveling down the outside of the outer conductor is most effectively eliminated by using both the back-gap and choke sleeve.

CONCLUSIONS

The four variations of a coaxial line antenna approximated the radiation pattern of the standard two-wire dipole with different levels of closeness. Looking at desirable features of return loss, S_{11} (dB), versus frequency and the far-field radiation pattern, some antennas performed better than others. For ease of comparison, the simulated and measured radiation patterns of all of the antennas have been presented. As seen, all three of the modifications on the extended inner conductor antenna approximated a 2-D slice of the typical doughnut shape of the two-wire dipole. However, the far-field radiation pattern of the combined choke-sleeve and back-gap antenna came closest to that of the two-wire dipole antenna.

Since the return loss, or S_{11} (dB), is directly related to the fraction of incident power that is radiated, a figure of merit or quality factor for an antenna may be expressed as the product of return loss and the frequency band or bandwidth over which an average value of return loss occurs. The magnitude of this product of return loss and bandwidth is the area under the curve of S_{11} (dB) versus frequency. This product, frequency bandwidth times return loss, is estimated over the 2.5 to 5 GHz band for each antenna as

Extended inner conductor antenna:
 $2.5 \times \text{RL} = 12.5$

TECHNICAL FEATURE

Back-gap antenna: $2.5 \times RL = 36.5$
Choke-sleeve antenna: $2.5 \times RL = 33$
Back-gap + choke-sleeve antenna: $2.5 \times RL = 27$.

Using this basis for comparison, the back-gap antenna is the best performer, and the extended inner conductor antenna is the worst (as expected). Again, no attempt was made to improve the impedance match of any of the antennas.

Figures 8 and 9 show the simulated input reactance and resistance, respectively, of a two-wire dipole, a quarter-wavelength spaced back-gap and a choke-sleeve antenna. Of the three, the choke-sleeve antenna appears to be most promising for additional optimization since the reactance remains near zero and the radiation resistance remains constant over a range of frequencies above and below where $2L \Rightarrow \lambda$. This implies that this antenna could be impedance matched to a 50Ω source over a broad range of frequencies.

Finally, while it was assumed throughout that the antennas are radiating into air, they may well be used to radiate into biological tissue or some other medium. As an interstitial applicator for hyperthermia cancer therapy, the surrounding medium may be composed of a thin layer of air, a thin layer of plastic catheter and a large mass of biological tissue. Also, for hyperthermia cancer therapy, the antennas may be external to the patient and radiate into a thin layer of plastic, a larger layer of deionized water (as a cooling bolus) and a large mass of biological tissue.

For illustration, assume that the combination of all surrounding materials yields an effective permittivity of $\epsilon = 49\epsilon_0$, where $\epsilon_0 = 8.854 \text{ pF/m}$ (the value for air or vacuum). This will change two parameters: both the antenna input impedance and the wave propagation velocity in the surrounding medium will be reduced by the square root of 49. Consequently, the values of reactance and resistance will be divided by 7. Also, the wavelength (λ) will be reduced by a factor of 7, and since $L = \lambda/4$, the physical length L is reduced by a factor of 7 for the same operating frequency. Conversely, if λ is made longer by a factor of 7 (operating frequency reduced by a factor of 7), the physical length (L) would be kept the same as in air and still be $\lambda/4$ at the reduced operating frequency. ■

ACKNOWLEDGMENTS

The authors express their deep appreciation to Esther Drozd and Guining Shi for the valuable help that they contributed in preparing this paper. This work was supported in part by NIH/NCI Grant number 2PO1 CA42745-16.

References

1. W.L. Stutzman and G.A. Theile, *Antenna Theory and Design*, John Wiley & Sons Inc., Somerset, NJ, 1981.
2. E.C. Jordan, *Electromagnetic Waves and Radiating Systems*, Prentice-Hall, Englewood Cliffs, NJ, 1950.
3. R.G. Brown, R.A. Sharpe, W.L. Hughes and R.E. Post, *Lines, Waves and Antennas, the Transmission of Electric Energy*, Ronald Press, New York, NY, 1961.
4. User's Manual, HP High Frequency Structure Simulator, Hewlett Packard Co., Palo Alto, CA, 1997.
5. T.S.M. Maclean, *Principles of Antennas: Wire and Aperture*, Cambridge University Press, New York, NY, 1986.
6. C.A. Balanis, *Antenna Theory: Analysis and Design*, Second Edition, John Wiley and Sons Inc., Somerset, NJ, 1997.
7. S.B. Cohn, "Characteristic Impedance of the Shielded-strip Transmission Line," *IEEE Transactions on Microwave Theory and Techniques*, Vol. 2, July 1954, pp. 52-57.
8. M.A. Plonus, *Applied Electro-magnetics*, McGraw-Hill, New York, NY, 1978.

R. Brian Drozd received his BSEE degree from the University of North Carolina at Charlotte. After graduation, he became a graduate research assistant at Duke University, under the supervision of Dr. William T. Joines, where he studied microwaves and electromagnetics. After graduating with a MSEE degree, he worked as a research engineer at Industrial Microwave Systems (IMS), while also obtaining a master's of engineering management degree (MEM) from Duke. Currently, he is a patent engineer at Intellectual Property/Technology Law (IPTL) in Chapel Hill, NC, assisting IPTL in the preparation, prosecution and correction of patents and patent applications.

William T. Joines received his BSEE degree from North Carolina State University, Raleigh, NC, and his MS and PhD degrees in electrical engineering from Duke University, Durham, NC. He was a member of the technical staff at Bell Telephone Laboratories, doing research and development of microwave components and systems for military applications, and is now a professor of electrical and computer engineering at Duke. His research and teaching interests include electromagnetic wave interactions with structures and materials, mainly at microwave and optical frequencies. He is the author of more than 100 technical papers on electromagnetic wave theory and applications, and the holder of twelve US patents.

TECHNICAL FEATURE

